

# A Correlation Information-based Spatiotemporal Network for Traffic Flow Forecasting

Weiguo Zhu, Yongqi Sun\*, Xintong Yi, Yan Wang  
 School of Computer and Information Technology, Beijing Jiaotong University  
 Beijing Key Lab of Traffic Data Analysis and Mining  
 Beijing, China  
 {zhuweiguo, yqsun, xintongyi, yan.wang}@bjtu.edu.cn

## ABSTRACT

With the growth of transport modes, high traffic forecasting precision is required in intelligent transportation systems. Most previous works utilize the transformer architecture based on graph neural networks and attention mechanisms to discover spatiotemporal dependencies and dynamic relationships. The correlation information among spatiotemporal sequences, however, has not been thoroughly considered. In this paper, we present two elaborate spatiotemporal representations, spatial correlation information (SCorr) and temporal correlation information (TCorr), among spatiotemporal sequences based on the maximal information coefficient. Using SCorr, we propose a novel correlation information-based spatiotemporal network (CorrSTN), including a dynamic graph neural network component incorporating correlation information into the spatial structure effectively and a multi-head attention component utilizing spatial correlation information to extract dynamic temporal dependencies accurately. Using TCorr, we further explore the correlation pattern among different periodic data and then propose a novel data selection scheme to identify the most relevant data. The experimental results on the highway traffic flow (PEMS07 and PEMS08) and metro crowd flow (HZME inflow and outflow) datasets demonstrate that CorrSTN outperforms the state-of-the-art methods in terms of predictive performance. In particular, on the HZME (outflow) dataset, our model makes significant improvements compared with the latest model ASTGNN by 12.7%, 14.4% and 27.4% in the metrics of MAE, RMSE and MAPE, respectively.

## CCS CONCEPTS

• Information systems → Data mining; Spatial-temporal systems.

## KEYWORDS

Correlation, Feature extraction, Forecasting, Attention, Graph neural network, Predictive models

\* Corresponding author.  
 E-mail address: yqsun@bjtu.edu.cn (Y. Sun).

Permission to make digital or hard copies of all or part of this work for personal or classroom use is granted without fee provided that copies are not made or distributed for profit or commercial advantage and that copies bear this notice and the full citation on the first page. Copyrights for components of this work owned by others than ACM must be honored. Abstracting with credit is permitted. To copy otherwise, or republish, to post on servers or to redistribute to lists, requires prior specific permission and/or a fee. Request permissions from permissions@acm.org.  
 Conference acronym 'XX, June 03–05, 2018, Woodstock, NY

© 2022 Association for Computing Machinery.  
 ACM ISBN 978-1-4503-XXXX-X/18/06...\$15.00  
<https://doi.org/XXXXXXX.XXXXXXX>

## ACM Reference Format:

Weiguo Zhu, Yongqi Sun\*, Xintong Yi, Yan Wang. 2022. A Correlation Information-based Spatiotemporal Network for Traffic Flow Forecasting. In *Proceedings of Make sure to enter the correct conference title from your rights confirmation email (Conference acronym 'XX)*. ACM, New York, NY, USA, 11 pages. <https://doi.org/XXXXXXX.XXXXXXX>

## 1 INTRODUCTION

The construction of smart cities externally requires diverse transportation modes and internally relies on a dependable intelligent transportation system (ITS). As one of the most fundamental and crucial techniques in smart city construction, traffic forecasting has become a hot research topic. Due to the massive and complex structural spatiotemporal data in ITSs, how to precisely predict the traffic flow using these data has become the top priority.

Traffic flow forecasting utilizes historical traffic data to predict future flow timestamps. Early works focusing on time series prediction have produced excellent results. Traditional methods, such as SVR [5], SVM [12, 20] and KNN [17, 21], have been extensively applied to traffic forecasting. However, these methods need to identify the data characteristics and ignore the spatial features.

With the rapid development of deep learning, deep neural networks have been used to extract spatiotemporal features for traffic forecasting. The convolutional neural network (CNN) is introduced into traffic forecasting tasks as an effective method to extract spatial features [4, 23, 27, 29]. However, these methods are coarse-graining processes utilizing CNN to capture neighbor block attributes and extract nonlinear spatial dependencies by a grid representation.

Considering that the grid representation cannot adequately represent the flow between sensors, graph representation is proposed to encode the elaborate relationships among sensors [14, 28]. In recent years, the graph neural network (GNN), as an efficient and effective method, has gradually become the essential traffic prediction module for graph representation. GNN-based methods concentrate on the relationships among adjacent sensors to aggregate sequence attributes [7, 8, 13, 14, 19, 28]. Furthermore, attention-based methods, such as [7, 8, 13, 15, 19, 24, 31], demonstrate the ability of long-term traffic flow forecasting and pattern learning by using queries, keys and values triples to calculate the interrelationships between different timestamps.

Nevertheless, two key issues need to be paid more attention. On the one hand, for graph neural networks, each sensor is defined as a node, and each spatial road is defined as an edge. These methods aggregate neighbor node features by GNN with the predefined graph structure. However, the neighbor sensors do not usually have a similar pattern, which does not meet the GNN assumption.

Researchers have made efforts to take mixed-hop propagation to explore deep neighborhoods [25], the DTW algorithm to construct a graph matrix [6, 13], and dynamic graph convolution to capture dynamic relationships [9, 30]. Although these methods make considerable improvements for traffic forecasting, their performance could be increased if they take the elaborate and density correlation information into consideration. On the other hand, the attention mechanism is designed to extract the discrete language feature relationships, which does not take the stable contextual features into account for continuous data.

In this paper, to solve the above two issues, we first introduce a spatial correlation representation (**SCorr**) to elaborately reflect the relevant features among temporal sequences. Based on SCorr, a dynamic correlation information GNN (**CIGNN**) is designed to integrate the spatial graph network with SCorr and capture comparable patterns from each sensor with different weights. In addition, to handle the unstable contextual features in the attention mechanism, we propose a correlation information multi-head attention (**CIATT**), which can stabilize contextual features by aggregating the top- $k$  comparable patterns from different sensors and offer the most relevant sequence pattern as a match template. With correlation information, we propose an effective correlation information-based spatiotemporal network for traffic flow forecasting (**CorrSTN**), which employs CIGNN to discover the dynamic spatial dependencies in traffic flow datasets and CIATT to match the relevant temporal traffic patterns. Finally, similar to SCorr, we build a temporal correlation information representation (**TCorr**) for neural network-based methods, which can mine the relevant sequence among different timeline segments and provide an effective data selection scheme for time-series forecasting tasks.

For traffic flow forecasting, we summarize four key contributions of our work as follows:

- We propose an elaborate spatial correlation information representation formed as a density correlative matrix.
- In our model, we propose a dynamic correlation information GNN to overcome the shortcomings of the predefined graph structure and provide comparable patterns for each sensor to learn. Meanwhile, to the best of our knowledge, we are the first to apply correlation information to the attention mechanism, which further supplies a more stable mechanism for continuous data.
- We are the first to propose a representation of temporal correlation information for neural network-based methods to supply an efficient data selection scheme for time-series forecasting tasks.
- The experimental results on four real-world datasets show that the predictive performance of CorrSTN outperforms fifteen baseline models.

## 2 PRELIMINARIES

**Definition 1.** Traffic Network. We define a traffic network as a directed or an undirected graph  $G = (V, E)$ , where  $V$  is a set of  $|V| = N$  nodes, each node represents a traffic sensor, and  $E$  is a set of edges.

**Definition 2.** Traffic spatiotemporal sequence. We define a traffic spatiotemporal sequence as  $X = (X^1, X^2, \dots, X^T) \in \mathbb{R}^{T \times N \times C}$

, where  $X^t = (x_1^t, x_2^t, \dots, x_N^t) \in \mathbb{R}^{N \times C}$  denotes the vector of the  $N$  sensors with  $C$  attributes at timestamp  $t$ .

**Definition 3.** Periodic Data. We define the hourly, daily and weekly data intervals as  $T_h$ ,  $T_d$  and  $T_w$ , respectively. Given time window  $\tau$ , the historical periodic data can be defined as

$$X = (X^{t-T_w+1}, X^{t-T_w+2}, \dots, X^{t-T_w+\tau}, \\ X^{t-T_d+1}, X^{t-T_d+2}, \dots, X^{t-T_d+\tau}, \\ X^{t-T_h+1}, X^{t-T_h+2}, \dots, X^{t-T_h+\tau}), \quad (1)$$

where the time interval of each timestamp is 5 minutes on the datasets, and  $\tau = 12$  in this paper.

**Problem 1.** Given the historical periodic data  $X \in \mathbb{R}^{T_{hdw} \times N \times C}$  defined as Equation (1), where  $T_{hdw} \in [\tau, 2\tau, 3\tau]$  will change according to our periodic data selection scheme for different datasets. Then our focus is to predict traffic flow for all sensors over the next  $L$  timestamps,

$$f(X) \rightarrow (\hat{X}^{t+1}, \hat{X}^{t+2}, \dots, \hat{X}^{t+L}) \in \mathbb{R}^{L \times N \times 1}, \quad (2)$$

where  $f(\cdot)$  is the mapping function aimed at learning learn and  $L = 12$  in our model.

## 3 METHODOLOGY

In this section, we will introduce our spatiotemporal correlation information representations (SCorr and TCorr) and the correlation information-based components (CIGNN and CIATT). The overall framework of CorrSTN is based on an encoder-decoder architecture, as shown in Figure 1. The encoder (decoder) network consists of temporal position embedding, spatial position embedding and encoder (decoder) layer components. The CIGNN and CIATT components are connected by the residual connection and layer normalization in each encoder and decoder layer. The second CIATT component of each decoder layer is designed to receive the encoder output as historical memory.

### 3.1 Spatiotemporal Correlation Information Representation

In this subsection, we propose two elaborate spatiotemporal representations based on the maximal information coefficient [18], spatial correlation information (SCorr) and temporal correlation information (TCorr). To measure the degree of correlation information among sensor sequences, the maximal information coefficient (MIC) method is employed in the two spatiotemporal representations. Compared with DTW and cosine similarity methods, MIC not only can capture a wide range of associations but also enables fast calculations.

To explain the calculation process of MIC in detail, we first define two sequences, i.e.  $var_1 \in \mathbb{R}^M$  and  $var_2 \in \mathbb{R}^M$ . By partitioning the  $x$ -axis into  $A$  parts and the  $y$ -axis into  $B$  parts, the degree of correlation information between  $var_1$  and  $var_2$  can be calculated as follows,

$$MIC(var_1, var_2) = \frac{\max_{A \times B < M^2} \{I_{a,b}(var_1, var_2)\}}{\log_2 \min\{A, B\}}, \quad (3)$$

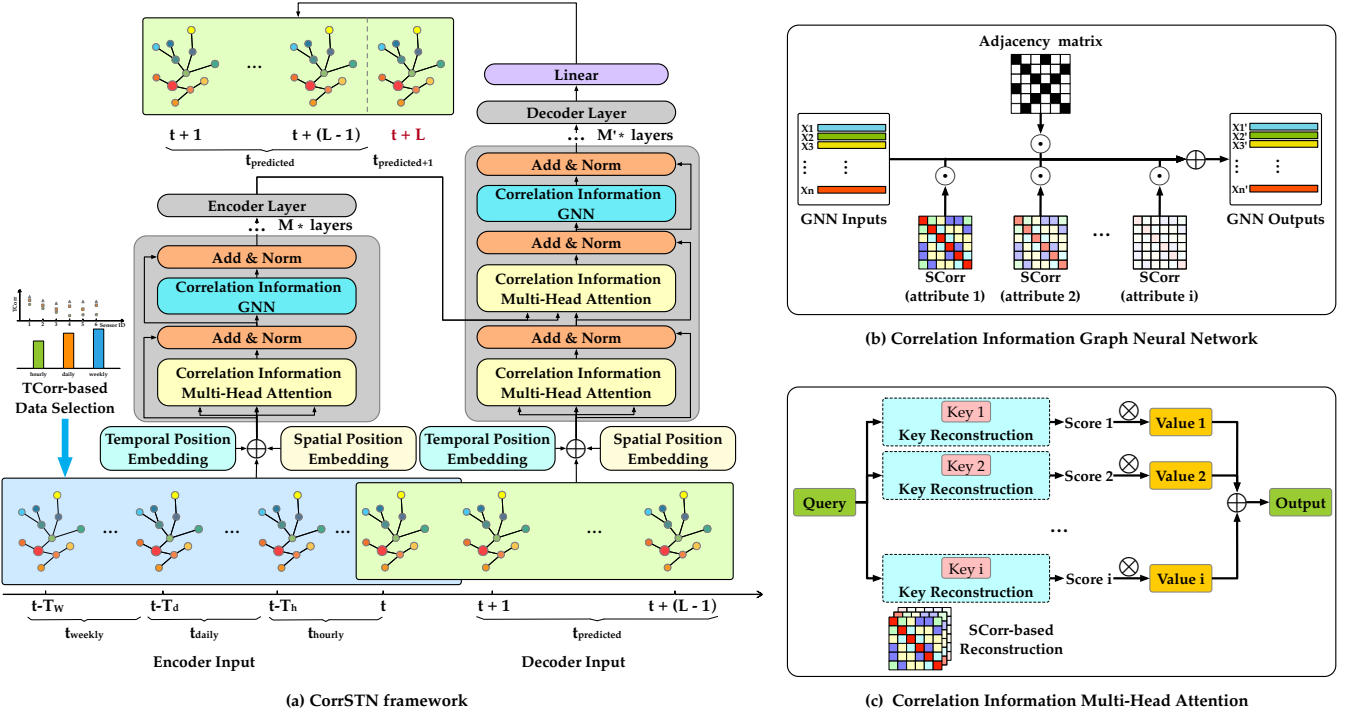


**Figure 1: An illustration of the proposed framework. (a) Left: The CorrSTN framework. The framework is a transformer network based on the encoder-decoder architecture. Each encoder (decoder) layer contains a (two) correlation information multi-head attention component(s) and a correlation information GNN component. (b) Upper right: Details of the correlation information graph neural network component. (c) Lower right: Details of the correlation information multi-head attention component.**

where  $\eta$  is a parameter to control the number of partitions and  $I_{a,b}$  denotes the mutual information.  $I_{a,b}$  is calculated as follows,

$$I_{a,b} = \sum_{a < A, b < B} q(a,b) \log_2 \left( \frac{q(a,b)}{q(a)q(b)} \right),$$

where  $q(a,b)$  is the joint probability density and  $q(a)$  and  $q(b)$  are the edge probability densities when choosing the  $(a,b)$  grids.

**3.1.1 Spatial Correlation Information.** In traffic forecasting tasks, the sequence of input data shows interrelated spatial characteristics. In this subsection, we propose SCorr to represent the dependence among spatiotemporal sensor sequences based on MIC.

Let  $X_i^c$  denote the sensor  $i$  vector with attribute  $c$  of  $T$  timestamps. Then, SCorr is defined as follows,

$$\text{SCorr}(X)_{i,j}^c = \text{MIC}(X_i^c, X_j^c), \quad (4)$$

where  $\text{SCorr}(X) \in \mathbb{R}^{N \times N \times C}$  is the degree of correlation information, and  $\text{SCorr}(X)_{i,j}^c \in [0, 1]$  denotes the degree of correlation information between sensor  $i$  and sensor  $j$  in attribute  $c$ .

Concretely, as shown in Figure 2(a), the data sequences with  $T$  timestamps are shown. We select the upper and lower sensor sequences to calculate the degree of correlation information as one example. According to Equation (4), we calculate the degree for each sensor pair, and then the SCorr matrices are shown in Figure 2(b).

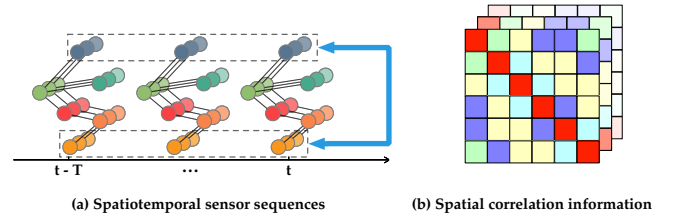


**Figure 2: An illustration of the SCorr calculation.**

Generally, each sensor has varying correlative relationships with other sensors in the traffic road or station network. The sparse adjacency matrix cannot represent it just by 1 or 0. In contrast, the SCorr matrices are elaborate and density spatiotemporal representations with values ranging from 0 to 1. High values signify strong correlative relationships and similar patterns between sensors, while low values express large differences and low reference values.

**3.1.2 Temporal Correlation Information.** There also exist different temporal associations among each temporal sequence in the traffic flow data. Thus, in this subsection, similar to SCorr, we propose an effective and efficient representation, called TCorr, to explore the similar pattern among different timeline segments and catch the most relevant data for any traffic forecasting task. Actually, TCorr can be used to explore associations of any timeline segments. In

this paper, we only focus on periodic data, including hourly, daily and weekly data.

Let  $X_{hourly} \in \mathbb{R}^{\tau \times N \times C}$  (resp.  $X_{daily}$ ,  $X_{weekly}$ ) denotes the vector of the last hour (resp. day, week) before the predicted data  $\tilde{X} \in \mathbb{R}^{\tau \times N \times C}$ . Then, TCorr is defined as follows,

$$\text{TCorr}(X)_i^c = \frac{1}{T} \sum_{t=1}^T \text{MIC}(X_{i,t}^{c,t+\tau}, \tilde{X}_{i,t}^{c,t+\tau}), \quad (5)$$

where  $\text{TCorr}(X) \in \mathbb{R}^{N \times C}$  is the degree of temporal correlation information,  $\text{TCorr}(X)_i^c \in [0, 1]$  denotes the degree of temporal correlation information of sensor  $i$  with attribute  $c$ , and  $X_{i,t}^{c,t+\tau}$  denotes the vector of sensor  $i$  with attribute  $c$  between timestamp  $t$  and timestamp  $t + \tau$  of  $X_{hourly}$ ,  $X_{daily}$  or  $X_{weekly}$ . Considering the uncertain factors, we set different weights for different periodic types of data as follows,

$$\begin{aligned} \text{TCorr}_h &= \alpha \text{TCorr}(X_{hourly}) \\ \text{TCorr}_d &= \beta \text{TCorr}(X_{daily}) \\ \text{TCorr}_w &= \gamma \text{TCorr}(X_{weekly}), \end{aligned} \quad (6)$$

where the weights  $\alpha$ ,  $\beta$  and  $\gamma$  are set at 0.95, 0.95 and 0.85 in this paper, respectively. To verify the contribution of each periodic type, we define  $\Delta_{hd}$ ,  $\Delta_{hw}$  and  $\Delta_{dw}$  as follows,

$$\begin{aligned} \Delta_{hd}^c &= \frac{1}{N} \sum_{i=1}^N \text{TCorr}_{d,i}^c - \frac{1}{N} \sum_{i=1}^N \text{TCorr}_{h,i}^c \\ \Delta_{hw}^c &= \frac{1}{N} \sum_{i=1}^N \text{TCorr}_{w,i}^c - \frac{1}{N} \sum_{i=1}^N \text{TCorr}_{h,i}^c \\ \Delta_{dw}^c &= \frac{1}{N} \sum_{i=1}^N \text{TCorr}_{w,i}^c - \frac{1}{N} \sum_{i=1}^N \text{TCorr}_{d,i}^c, \end{aligned} \quad (7)$$

where  $\Delta_{hd}^c$  (resp.  $\Delta_{hw}^c$ ,  $\Delta_{dw}^c$ ) denotes the gap of contribution between hourly and daily (resp. hourly and weekly, daily and weekly) data with attribute  $c$ .

According to Occam's Razor principle, the hourly data are included as the basis of the input data to provide the short-term tendency. Then, the daily (weekly) data are combined into input data if  $\Delta_{hd}^c > 0$  ( $\Delta_{hw}^c > 0$ ). When  $\Delta_{hd}^c > 0$  and  $\Delta_{hw}^c > 0$ , we select the periodic data to combine with input data as follows,

$$\text{periodic data} = \begin{cases} \text{daily and weekly data,} & \text{for } \Delta_{dw}^c > 0, \\ \text{daily or weekly data,} & \text{for } \Delta_{dw}^c = 0, \\ \text{daily data,} & \text{for } \Delta_{dw}^c < 0. \end{cases} \quad (8)$$

Figure 3(a) illustrates the calculation between the last hour (day, week) and the predicted data. Figure 3(b) includes the scatter chart for each sensor based on  $\text{TCorr}(X)$ , and the histogram based on the averaged degree of temporal correlation information of all sensors. We can see that  $\Delta_{hd}^c > 0$ ,  $\Delta_{hw}^c > 0$  and  $\Delta_{dw}^c > 0$ , thus, the hourly, daily and weekly data are the most relevant data for the traffic flow forecasting task.

For different dataset types, by using TCorr, the most relevant data with similar patterns data can be selected and combined as the most suitable data for any traffic flow forecasting task. We will discuss TCorr in Section 4.4 in depth.

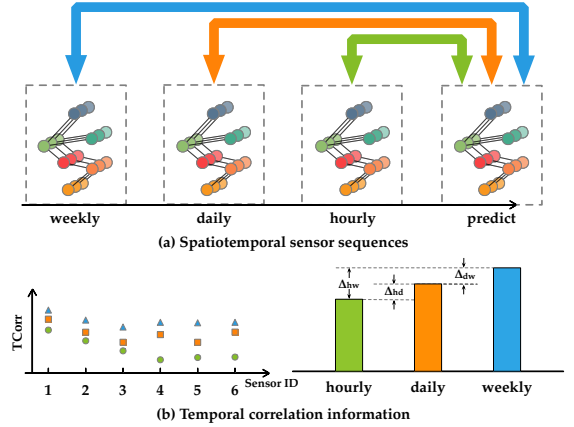


Figure 3: An illustration of the TCorr calculation.

### 3.2 Correlation Information Graph Neural Network

In this subsection, we propose a correlation information graph neural network (CIGNN) incorporating the spatial correlation information into the structure network, as shown in Figure 1(b). The original graph neural network is defined as follows,

$$\mathbf{Z}^{(l)} = \sigma \left( \mathbf{A} \mathbf{Z}^{(l-1)} \mathbf{W}^{(l)} \right), \quad (9)$$

where  $\mathbf{Z}^{(l)}$  and  $\mathbf{Z}^{(l-1)} \in \mathbb{R}^{N \times d_{model}}$ ,  $\mathbf{W}^{(l)} \in \mathbb{R}^{d_{model} \times d_{model}}$ , and  $\sigma$  are the sensor feature representation output and the input of  $d_{model}$  dimensions, linear projection weight matrix, and nonlinear activation function, respectively.  $l$  and  $l-1$  denote the layer number.  $\mathbf{A} \in \mathbb{R}^{N \times N}$  denotes the normalized structural adjacency matrix by the Laplacian regularization

$$\mathbf{A} = \tilde{\mathbf{D}}^{-\frac{1}{2}} \tilde{\mathbf{A}} \tilde{\mathbf{D}}^{-\frac{1}{2}},$$

where  $\tilde{\mathbf{A}} \in \mathbb{R}^{N \times N}$  is the graph adjacency matrix and  $\tilde{\mathbf{D}}$  is the diagonal matrix with the  $i_{th}$  element  $\tilde{D}_{ii} = \sum_j \tilde{A}_{ij}$ .

According to Equation (9), the network only considers the neighbor sensor relationships, even if the sensors do not have similar features and patterns. Aiming to widely capture similar patterns from other sensor nodes, we propose the CIGNN module as follows:

$$\hat{\mathbf{Z}}^{(l)} = \sum_{c=1}^C \psi_c \sigma \left( \mathbf{SCorr}_c \mathbf{S}_w \mathbf{Z}^{(l-1)} \mathbf{W}^{(l)} \right) \quad (10)$$

where  $\mathbf{SCorr}_c \in \mathbb{R}^{N \times N}$  denotes our proposed spatial correlation information in dimension  $c$ , and  $\psi_c$  are the trainable parameters to control the aggregation level of each attribute. To cover the dynamic change among sensors over time, we add a spatial dynamic weight matrix  $\mathbf{S}_w$  to adaptively adjust the degree of correlation information as in [8]. The spatial dynamic weight matrix is calculated as follows,

$$\mathbf{S}_w = \text{softmax} \left( \frac{\mathbf{Z}^{(l-1)} \mathbf{Z}^{(l-1)T}}{\sqrt{d_{model}}} \right) \in \mathbb{R}^{N \times N}. \quad (11)$$

Finally, we integrate the predefined graph structure to avoid losing local information by a trainable parameter  $\Omega$  as follows,

$$\hat{\mathbf{Z}}^{(l)} = \text{AGG}(\hat{\mathbf{Z}}^{(l)}, \Omega \mathbf{Z}^{(l)}), \quad (12)$$

Compared with previous works, the CIGNN module integrates correlation information and structural information, provides an accurate and dense interconnection network, and improves the efficiency of feature data aggregation between similar sensors.

### 3.3 Correlation Information Multi-Head Attention

In this subsection, we propose a correlation information multi-head attention (CIATT) component utilizing spatial correlation information to construct stable contextual features and extract dynamic temporal dependencies for continuous data, as shown in Figure 1(c).

Currently, many works use the attention mechanism for traffic flow forecasting. The attention mechanism, as the major component of transformer architecture, utilizes the queries ( $\mathbf{Q}$ ), keys ( $\mathbf{K}$ ), and values ( $\mathbf{V}$ ) as the inputs to model the dependencies of time points among sequences and construct a new embedding representation output as follows,

$$\text{Attention}(\mathbf{Q}, \mathbf{K}, \mathbf{V}) = \text{Softmax}\left(\frac{\mathbf{Q}\mathbf{K}^T}{\sqrt{d_{\text{head}}}}\right)\mathbf{V}, \quad (13)$$

where  $\mathbf{Q} \in \mathbb{R}^{N \times L_Q \times d_{\text{head}}}$ ,  $\mathbf{K} \in \mathbb{R}^{N \times L_K \times d_{\text{head}}}$ ,  $\mathbf{V} \in \mathbb{R}^{N \times L_V \times d_{\text{head}}}$  and  $d_{\text{head}}$  is the input dimension of one head.

However, the attention mechanism has excellent performance for discovering the associations by scattering the continuous traffic sequences as discrete time points, which threatens the stability and reduces associations between adjacent time points. To address the problem, we define the CIATT component as follows,

$$\text{CIATT}(\mathbf{Q}, \mathbf{K}, \mathbf{V}) = \text{Linear}(\text{Cat}(\text{CIATT}_1, \dots, \text{CIATT}_H)), \quad (14)$$

where there are  $H$  heads for the CIATT component, and the outputs of all heads are concatenated and reweighted by the Cat and Linear operators. The  $h_{th}$  head is defined as follows,

$$\text{CIATT}_h = \text{Softmax}\left(\frac{\mathbf{Q}_{(h)}\tilde{\mathbf{K}}_{(h)}^T}{\sqrt{d_{\text{head}}}}\right)\mathbf{V}_{(h)}. \quad (15)$$

Considering that different sensors with strong correlation information have similar patterns in the traffic road network, we construct  $\tilde{\mathbf{K}}_{(h)}$  by using SCorr to combine similar patterns of correlative sensors as follows,

$$\tilde{\mathbf{K}} = \mathcal{F}(\text{SCorr}, \mathbf{K}) = \frac{1}{C} \sum_{c=1}^C \text{SCorr}_c^T \hat{\mathbf{K}}, \quad (16)$$

where  $\mathcal{F}$  is the reconstruction function. The inputs are the spatial correlation information and original keys and the output  $\tilde{\mathbf{K}} \in \mathbb{R}^{N \times L_K \times d_{\text{head}}}$  is a more stable and reliable representation for the attention mechanism, where  $L_K$  is the length of  $\mathbf{K}$ . According to the degree of correlation information, the top  $U$  items are selected from SC and normalized via the softmax function as

$$\text{SCorr}_{i,m}^c = \frac{\exp(\text{SCorr}_{i,m}^c)}{\sum_{u=1}^U \exp(\text{SCorr}_{i,u}^c)},$$

and  $\hat{\mathbf{K}} \in \mathbb{R}^{N \times U \times L_K \times d_{\text{head}}}$  are the items selected from  $\mathbf{K}$  in the same order. In detail, the  $\tilde{\mathbf{K}}_i$  of sensor  $i$  in  $\tilde{\mathbf{K}}$  is calculated as follows,

$$\tilde{\mathbf{K}}_i = \frac{1}{C} \sum_{c=1}^C \sum_{u=1}^U \text{SCorr}_{i,u}^c \hat{k}_{i,u},$$

where  $\hat{k}_{i,u} \in \mathbb{R}^{L_K \times d_{\text{head}}}$  is the element of sensor  $i$  in  $\hat{\mathbf{K}}$ . Finally, we obtain the stable and reliable representation  $\tilde{\mathbf{K}} \in \mathbb{R}^{N \times L_K \times d_{\text{head}}}$  and its dimension is the same as that of  $\mathbf{K} \in \mathbb{R}^{N \times L_K \times d_{\text{head}}}$ .

Our method aggregates similar patterns from different sensors with SCorr weights and constructs more stable contextual features as keys ( $\tilde{\mathbf{K}}$ ) for the attention mechanism, which makes each time point able to accurately match the most relevant sequence pattern and achieve more precision for traffic flow forecasting.

### 3.4 Encoder-Decoder

The encoder-decoder is the basic architecture of the transformer network. In this paper, the input data of the encoder are the periodic data defined as Equation (1). The encoder input data are  $\mathbf{X} = (\mathbf{X}_{t_{\text{weekly}}}, \mathbf{X}_{t_{\text{daily}}}, \mathbf{X}_{t_{\text{hourly}}})$ , which are combined with the spatial position embedding and temporal position embedding. Then, CIATT constructs more stable contextual features and CIGNN integrates correlation information with structural information to learn the similar pattern for each sensor node, which are connected by the residual connection and layer normalization in each layer. The decoder input data are  $\mathbf{X} = (\mathbf{X}_t, \mathbf{X}_{t+1}, \dots, \mathbf{X}_{t+L-1})$ , which are processed as the encoder input. Furthermore, the decoder layer receives the encoder output as historical memory for prediction. Finally, the output data are  $\mathbf{X} = (\hat{\mathbf{X}}_{t+1}, \hat{\mathbf{X}}_{t+2}, \dots, \hat{\mathbf{X}}_{t+L})$ .

## 4 EXPERIMENTS

In this section, we conduct experiments to evaluate the performance of CorrSTN on four real-world spatiotemporal traffic network datasets and discuss the effect of each component. We partition each dataset into training, validation and test sets in a ratio of 6:2:2 by timestamps, and all data are normalized into  $[-1, 1]$  by the min-max method. In SCorr and TCorr,  $\eta$  is set at 0.6 to control the number of partitions. We evaluate the performance of our model by the metrics of mean absolute error (MAE), root mean square error (RMSE) and mean absolute percentage error (MAPE).

### 4.1 Datasets

The details of the four traffic datasets are given in Table 1. The datasets of the first type are collected from two districts in California [3], namely, PEMS07 and PEMS08, which contain 883 and 170 nodes, respectively. The datasets of the second type are collected from the Hangzhou metro system [8], namely, HZME, including inflow and outflow datasets. The HZME datasets contain 80 nodes and 168 edges (undirected network) with a sparse spatial structural relationship.

Table 1: Datasets description.

data type	dataset	#sensors	time span
highway traffic flow	PEMS07	883	05/01/2017-08/31/2017
	PEMS08	170	07/01/2016-08/31/2016
metro crowd flow	HZME(inflow)	80	01/01/2019-01/26/2019
	HZME(outflow)	80	

**Table 2: Performance comparison on the datasets of highway traffic flow and metro crowd flow.**

Datasets (Highway Traffic Flow)	PEMS07			PEMS08		
Metrics	MAE	RMSE	MAPE(%)	MAE	RMSE	MAPE(%)
VAR (2003)	101.2	155.14	39.69	22.32	33.83	14.47
SVR (1997)	32.97 ± 0.98	50.15 ± 0.15	15.43 ± 1.22	23.25 ± 0.01	36.15 ± 0.02	14.71 ± 0.16
LSTM (1997)	29.71 ± 0.09	45.32 ± 0.27	14.14 ± 1.00	22.19 ± 0.13	33.59 ± 0.05	18.74 ± 2.79
DCRNN (2018)	23.60 ± 0.05	36.51 ± 0.05	10.28 ± 0.02	18.22 ± 0.06	28.29 ± 0.09	11.56 ± 0.04
STGCN (2018)	27.41 ± 0.45	41.02 ± 0.58	12.23 ± 0.38	18.04 ± 0.19	27.94 ± 0.18	11.16 ± 0.10
ASTGCN (2019)	25.98 ± 0.78	39.65 ± 0.89	11.84 ± 0.69	18.86 ± 0.41	28.55 ± 0.49	12.50 ± 0.66
GWN (2019)	21.22 ± 0.24	34.12 ± 0.18	9.07 ± 0.20	15.07 ± 0.17	23.85 ± 0.18	9.51 ± 0.22
GMAN (2020)	21.56 ± 0.26	34.97 ± 0.44	9.51 ± 0.16	15.33 ± 0.03	26.10 ± 0.28	10.97 ± 0.37
AGCRN (2020)	22.56 ± 0.33	36.18 ± 0.46	9.67 ± 0.14	16.26 ± 0.43	25.62 ± 0.56	10.33 ± 0.34
STSGCN (2020)	23.99 ± 0.14	39.32 ± 0.31	10.10 ± 0.08	17.10 ± 0.04	26.83 ± 0.06	10.90 ± 0.05
MTGNN (2020)	20.57 ± 0.61	33.54 ± 0.73	9.12 ± 0.13	15.52 ± 0.06	25.59 ± 0.29	13.56 ± 1.11
STFGNN (2021)	22.07 ± 0.11	35.80 ± 0.18	9.21 ± 0.07	16.64 ± 0.09	26.22 ± 0.15	10.60 ± 0.06
STGODE (2021)	22.89 ± 0.15	37.49 ± 0.07	10.10 ± 0.06	16.79 ± 0.02	26.05 ± 0.11	10.58 ± 0.08
DMSTGCN (2021)	20.77 ± 0.57	33.67 ± 0.54	8.94 ± 0.42	16.02 ± 0.10	26.00 ± 0.21	10.28 ± 0.08
ASTGNN (2021)	20.62 ± 0.12	34.00 ± 0.21	8.86 ± 0.10	15.00 ± 0.35	24.70 ± 0.53	9.50 ± 0.11
ASTGNN(p) (2021)	19.26 ± 0.17	32.75 ± 0.25	8.54 ± 0.19	12.72 ± 0.09	22.60 ± 0.13	8.78 ± 0.20
CorrSTN	19.62 ± 0.05	33.11 ± 0.23	8.22 ± 0.06	14.27 ± 0.17	23.67 ± 0.15	9.32 ± 0.06
CorrSTN(p)	<b>18.10 ± 0.10</b>	<b>31.61 ± 0.12</b>	<b>7.58 ± 0.12</b>	<b>12.56 ± 0.03</b>	<b>22.43 ± 0.03</b>	<b>8.53 ± 0.09</b>
Datasets (Metro Crowd Flow)	HZME(inflow)			HZME(outflow)		
Metrics	MAE	RMSE	MAPE(%)	MAE	RMSE	MAPE(%)
VAR (2003)	17.65	28.1	58.07	22.35	37.96	96.68
SVR (1997)	21.94 ± 0.02	40.73 ± 0.02	49.40 ± 0.07	25.59 ± 0.12	50.07 ± 0.17	91.71 ± 3.18
LSTM (1997)	22.53 ± 0.51	39.33 ± 0.35	60.12 ± 2.44	26.18 ± 0.32	48.91 ± 0.45	103.06 ± 8.52
DCRNN (2018)	12.25 ± 0.13	20.91 ± 0.33	25.53 ± 0.38	18.02 ± 0.16	31.45 ± 0.39	66.98 ± 1.65
STGCN (2018)	12.88 ± 0.28	22.86 ± 0.39	29.66 ± 1.50	19.12 ± 0.23	33.12 ± 0.36	73.66 ± 1.49
ASTGCN (2019)	13.10 ± 0.47	23.23 ± 0.81	33.29 ± 3.63	19.35 ± 0.51	33.20 ± 1.07	88.75 ± 4.00
GWN (2019)	11.20 ± 0.11	19.73 ± 0.46	23.75 ± 0.71	17.50 ± 0.12	30.65 ± 0.41	73.65 ± 2.72
GMAN (2020)	11.35 ± 0.20	20.60 ± 0.33	26.85 ± 0.72	18.03 ± 0.11	32.51 ± 0.37	74.57 ± 0.45
AGCRN (2020)	11.86 ± 0.71	24.39 ± 0.73	30.93 ± 1.82	19.34 ± 1.27	33.85 ± 1.16	88.85 ± 0.48
STSGCN (2020)	12.85 ± 0.10	23.20 ± 0.38	28.02 ± 0.19	18.74 ± 0.13	33.12 ± 0.43	76.85 ± 1.01
MTGNN (2020)	11.99 ± 0.39	20.57 ± 0.55	26.87 ± 0.64	18.79 ± 0.80	32.27 ± 0.60	87.63 ± 3.84
STFGNN (2021)	13.12 ± 0.23	23.02 ± 0.37	30.67 ± 0.53	18.90 ± 0.18	34.12 ± 0.43	77.32 ± 2.33
STGODE (2021)	11.36 ± 0.06	22.02 ± 0.14	40.50 ± 1.01	19.43 ± 0.38	33.67 ± 0.64	89.90 ± 2.57
DMSTGCN (2021)	12.64 ± 0.28	21.79 ± 0.53	28.21 ± 0.75	18.52 ± 0.37	32.26 ± 0.84	77.08 ± 0.76
ASTGNN (2021)	11.46 ± 0.08	20.84 ± 0.25	24.42 ± 0.30	17.94 ± 0.11	31.91 ± 0.32	72.46 ± 2.42
ASTGNN(p) (2021)	10.94 ± 0.04	18.89 ± 0.11	23.33 ± 0.14	17.47 ± 0.03	30.78 ± 0.08	70.52 ± 0.27
CorrSTN	11.20 ± 0.06	19.71 ± 0.14	24.04 ± 0.38	17.26 ± 0.08	30.66 ± 0.15	65.33 ± 0.26
CorrSTN(p)	<b>10.39 ± 0.10</b>	<b>17.23 ± 0.26</b>	<b>22.93 ± 0.35</b>	<b>15.24 ± 0.37</b>	<b>26.34 ± 0.70</b>	<b>51.22 ± 2.64</b>

## 4.2 Performance

We compare our model with fifteen baseline methods, including VAR [16], SVR [5], LSTM [11], DCRNN [14], STGCN [28], ASTGCN [7], GWN [26], GMAN [30], AGCRN [2], STSGCN [19], MTGNN [25], STFGNN [13], STGODE [6], DMSTGCN [9] and ASTGNN [8]. We repeat the experiments more than 5 times on all datasets to evaluate the performance of our model, and the means and standard deviations are collected in Table 2, where the bold font highlights the best values. The results obtained by using periodic data, including hourly, daily and weekly data are marked by (p).

Using only hourly data, CorrSTN achieves the best values in the metrics of MAE, RMSE and MAPE on the highway traffic flow and metro crowd flow datasets. With the input being periodic data (hourly, daily, weekly), the predictive performance of our model outperforms the state-of-the-art method ASTGNN(p). Especially on the HZME (outflow) dataset, our model CorrSTN outperforms the

latest model ASTGNN(p) by 12.7%, 14.4% and 27.4% in the metrics of MAE, RMSE and MAPE, respectively.

To clearly state the importance of correlation information, we compare CorrSTN with these methods without correlation information, including VAR, SVR, LSTM, DCRNN, STGCN, ASTGCN, STSGCN and ASTGNN. The neural network-based models achieve considerable improvement over traditional time-series models, which indicates that neural network-based and graph-based methods can effectively extract traffic flow features. Our model with correction information further enhances the forecasting ability and outperforms all methods on all datasets.

Now, we compare CorrSTN with the methods using correlation information, including GWN, GMAN, AGCRN, MTGNN, STFGNN, STGODE and DMSTGCN. As shown in Table 2, CorrSTN achieves the best values with the hourly data or with the periodic data on all datasets. Compared with the GWN, GMAN, and AGCRN, which

utilize the adaptive graph structure, the SCorr of our model can provide more elaborate and density correlation information for each sensor, and the CIGNN can effectively combine the SCorr with the spatial structure. Moreover, although STFGNN and STGODE adopt the DTW algorithm to construct a graph matrix to further learn the relationship among the sensors, the SCorr of our model makes full use of the MIC algorithm, which can capture a wider range of associations. In addition, the MTGNN and DMSTGCN use dynamic graph convolution to capture dynamic relationships, which are effective modules for traffic flow forecasting. In contrast, our module CIGNN utilizes a spatial dynamic weight matrix to cover each change in different locations and times, and CIATT matches the most relevant sequence pattern in the attention mechanism by weighting and aggregating similar patterns from different sensors.

Moreover, using TCrr, our model adopts the hourly and daily data as the whole training data, while ASTGNN adopts the hourly and weekly data on the HZME (outflow) dataset. In particular, our model makes significant improvements compared with the state-of-the-art model ASTGNN by 12.7%, 14.4% and 27.4% in the metrics of MAE, RMSE and MAPE, respectively. The result indicates that our TCrr can mine the relevant sequence among different timeline segments and provide an effective data selection scheme for traffic flow forecasting tasks.

In conclusion, by combining the correlation information with GNN by the CIGNN component, employing a stable and effective attention mechanism by the CIATT component and selecting the appropriate periodic data by using TCrr, our model can significantly improve the predictive performance.

### 4.3 Ablation Experiments

In this subsection, we verify the effectiveness of our CIGNN and CIATT components on the PEMS08 dataset. For comparison, we assign the state-of-the-art ASTGNN as the baseline. Moreover, *with*-CIGNN (*with*-CIATT) denotes the model using the CIGNN (CIATT) component, and CIGNN+CIATT denotes the model using CIGNN and CIATT components. We take the hourly data as input and show the predictive results for all prediction points, as shown in Figure 4. We find that *with*-CIGNN (resp. *with*-CIATT) outperforms the baseline by 1.04%, 0.72% and 1.50% (resp. 2.74%, 2.42% and 2.13%) in the

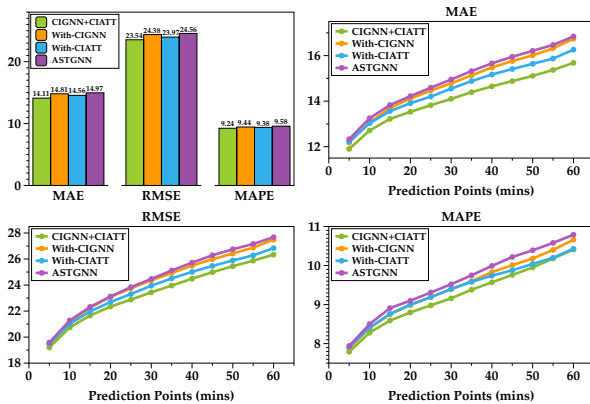


Figure 4: Ablation results on the PEMS08 dataset.

metrics of MAE, RMSE and MAPE, respectively. CIGNN+CIATT outperforms the baseline by 5.72%, 4.16% and 3.61% in the metrics of MAE, RMSE and MAPE, respectively. The experimental results show that the CIGNN and CIATT modules can achieve considerable improvements in predictive accuracy.

Furthermore, comparing the results in Figure 4, we find that the CIATT component effectively shows higher effectiveness than the CIGNN component in the traffic flow forecasting task. The main reason is the design of the stable and effective attention component by using SCorr and the construction of a new representation considering sensors with similar patterns. Compared with the baseline ASTGNN, the *with*-CIATT and CIGNN+CIATT models consider more similar patterns to supply a more stable attention mechanism for each time point.

### 4.4 Performance of temporal correlation information

In this subsection, we explore the efficient data selection scheme among different periodic data with TCrr. Then, we conduct experiments to verify the accuracy on the HZME (outflow) dataset with different periodic data selection schemes.

We represent the temporal correlation information as Equation (6). The PEMS07 and PEMS08 datasets are the highway traffic flow datasets, while the HZME inflow and outflow datasets are the metro crowd flow datasets. As shown in Figure 5 and Table 3, the weekly data have the highest degree of correlation with the prediction data on the highway traffic flow datasets, while the daily data have the highest degree of correlation with the prediction data on the metro traffic flow datasets.

It is reasonable that the highway traffic flow datasets are collected from the highway of California, which reflect the characteristics of long-distance travel, while the metro crowd flow datasets are collected from the metro in Hangzhou, which reflect the characteristics of short-distance travel. Because of these different characteristics, temporal correlation information has different representations in historical periodic data. A case study of four real-world datasets can be found in Section B.2.

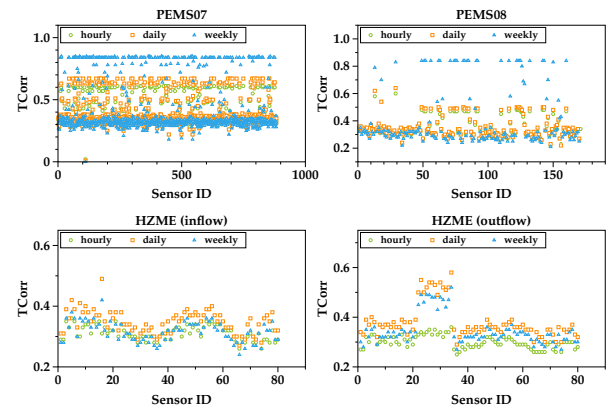


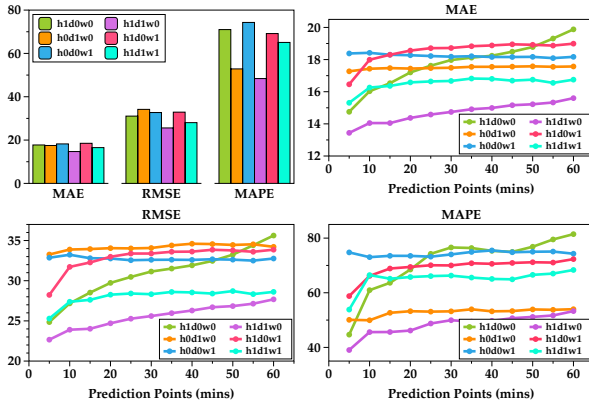
Figure 5: Temporal correlation information of each sensor on four datasets.



**Table 3: Temporal correlation information (average) on four datasets.**

	PEMS07	PEMS08	HZME(inflow)	HZME(outflow)
hourly	0.379	0.343	0.312	0.300
daily	0.397*	0.356*	<b>0.348</b>	<b>0.380</b>
weekly	<b>0.426</b>	<b>0.411</b>	0.316*	0.346*

The different TCorr representations on the four datasets indicate that different data selection schemes should be made for training. To verify the accuracy of these representations, we adopt six different input data selection schemes on the HZME (outflow) dataset, as shown in Figure 6, where  $h1$  ( $h0$ ),  $d1$  ( $d0$ ), and  $w1$  ( $w0$ ) denote that the input data (do not) contain hourly, daily and weekly data, respectively. The figures illustrate that the best model can be achieved with the  $h1d1w0$  scheme. Although the  $h1d1w1$  scheme contains more data for training, the data will lead to unstabilized contextual features. The results of different data selection schemes confirm that hourly and daily data are the appropriate input for CorrSTN on the HZME (outflow) dataset. Additionally, it verifies the correctness of TCorr and supplies the best data selection scheme to select the appropriate periodic data, as stated in Section 3.1.2.

**Figure 6: Results on the HZME (outflow) dataset with six different input data selection schemes.**

In summary, TCorr provides a reliable representation and an effective data selection scheme for periodic data. By the scheme, we select different periodic data for highway traffic flow and metro crowd flow data and achieve the best predictive performance of all baselines.

## 5 RELATED WORK

### 5.1 Traditional Traffic Forecasting Methods

The early works for traffic forecasting are based on machine learning methods. Drucker et al. propose a linear support vector machine (SVR) to predict traffic flow data in [5]. Lu et al. propose an advanced time series model based on vector autoregression (VAR) to capture the pairwise relationships among spatial sequences on traffic data in [16]. Hochreiter and Schmidhuber design the long short-term

memory (LSTM) network, a special RNN, to predict time series data and solve the vanishing gradient problem in [11]. With only temporal sequences considered and spatial relationships ignored, their prediction accuracy cannot satisfy the practical requirements.

### 5.2 Deep Neural Network Traffic Forecasting Methods

The deep neural network has dramatically improved traffic prediction accuracy by combining CNN and RNN variants. Li et al. propose a diffusion convolutional recurrent neural network (DCRNN) to employ a diffusion graph convolutional network and a gated recurrent unit (GRU) in seq2seq to predict traffic data [14]. Yu, Yin, and Zhu design a spatial-temporal graph convolutional network (STGCN) architecture for spatiotemporal datasets in the traffic forecasting task [28]. Wu et al. propose Graph WaveNet (GWN), which combines a graph convolution network with a temporal convolution network to capture spatial-temporal dependencies [26].

Since the attention mechanism can effectively model the dependencies among sequences, many works utilize it in traffic flow prediction tasks. Guo et al. present an ASTGCN model that uses spatial and temporal attention mechanisms to improve prediction accuracy [7]. Song et al. propose a spatial-temporal synchronous graph convolution network (STSGCN) to extract temporal adjacency features by considering the local spatiotemporal relation [19]. Recently, Guo et al. propose a GNN-based model ASTGNN [8] with the encoder-decoder architecture [22] and residual connection [10] and layer normalization [1] to learn the dynamics and heterogeneity of spatial-temporal graph data for traffic forecasting, which is an extension of their previous ASTGCN model. Its prediction accuracy is significantly improved by effectively capturing the local data trend and dynamically aggregating the spatial features.

Although these methods have achieved outstanding results, the prediction accuracy could be higher if the structural adjacency network for the GNN and attention mechanism components is used and the absolutely crucial correlation information among spatiotemporal sequences is considered.

### 5.3 Correlation Information Traffic Forecasting Methods

The GWN adopts an adaptive adjacency matrix as a supplement to the structural matrix by calculating the vector correlations during the training stage [26]. However, it cannot accurately reflect the correlation information by short-term sequences. Zheng et al. design a graph multi-attention network (GMAN) integrating spatial and temporal attention to capture sensor correlations [30]. Bai et al. propose adaptive graph generation to dynamic generate the graph during training in AGCRN [2]. Wu et al. make use of the graph learning layer in MTGNN to construct adaptive graph by multivariate node features [25]. Li and Zhu introduce a spatial-temporal fusion graph matrix combining the correlation information with the structural network (STFGNN). However, since the matrix is very sparse, the correlation among the sensors is not elaborate for traffic forecasting [13]. Fang et al. combine the spatial and semantic neighbors to consider spatial correlations in STGODE [6]. Han et al. propose a dynamic graph constructor and graph convolution



in DMSTGCN to learn the dynamic spatial dependencies as the extensive of predefined adjacency matrix [9].

## 6 CONCLUSION

In this paper, we propose a novel transformer-based network CorrSTN to predict traffic flow data in intelligent transportation systems. Considering the correlation information, we first propose two elaborate spatiotemporal representations named SCorr and TCorr for spatiotemporal sensor sequences. Then, by using SCorr, we design two crucial components named CIGNN and CIATT in our CorrSTN model. By using TCorr, we mine the correlations among different periodic data and design an effective data selection scheme for periodic datasets. Finally, we conduct experiments to verify each component and compare CorrSTN with fifteen baseline methods on the highway traffic flow and metro crowd flow datasets. The experimental results demonstrate that the CIGNN and CIATT components can effectively discover the spatial relationships and extract dynamic temporal dependencies, and the data selection scheme enables the appropriate data to further improve the prediction accuracy. Furthermore, the predictive performance of CorrSTN outperforms that of all other state-of-the-art methods.

## ACKNOWLEDGMENTS

This research is supported by the National Key R&D Program of China (No. 2021ZD0113002), National Natural Science Foundation of China (No. 61572005, 62072292, 61771058) and Fundamental Research Funds for the Central Universities of China (No. 2020YJS032). The support and resources from the Center for High Performance Computing at Beijing Jiaotong University is also gratefully acknowledged.

## REFERENCES

- [1] Jimmy Lei Ba, Jamie Ryan Kiros, and Geoffrey E Hinton. 2016. Layer normalization. *arXiv preprint arXiv:1607.06450* (2016).
- [2] Lei Bai, Lina Yao, Can Li, Xianzhi Wang, and Can Wang. 2020. Adaptive Graph Convolutional Recurrent Network for Traffic Forecasting. In *Advances in Neural Information Processing Systems (Advances in Neural Information Processing Systems, Vol. 33)*. 17804–17815.
- [3] Chao Chen, Karl Petty, Alexander Skabardonis, Pravin Varaiya, and Zhanfeng Jia. 2001. Freeway Performance Measurement System: Mining Loop Detector Data. *Transportation Research Record* 1748, 1 (2001), 96–102. <https://doi.org/10.3141/1748-12>
- [4] Zhiyong Cui, Ruimin Ke, and Yinhai Wang. 2018. Deep Bidirectional and Unidirectional LSTM Recurrent Neural Network for Network-Wide Traffic Speed Prediction. *CoRR* abs/1801.02143 (2018), 1–12.
- [5] Harris Drucker, Christopher J. C. Burges, Linda Kaufman, Alex Smola, and Vladimir Vapnik. 1997. Support Vector Regression Machines. In *Advances in Neural Information Processing Systems*, M. C. Mozer, M. Jordan, and T. Petsche (Eds.), Vol. 9. MIT Press.
- [6] Zheng Fang, Qingqing Long, Guojie Song, and Kunqing Xie. 2021. Spatial-Temporal Graph ODE Networks for Traffic Flow Forecasting. In *Proceedings of the 27th ACM SIGKDD Conference on Knowledge Discovery & Data Mining*. Association for Computing Machinery, New York, NY, USA, 364–373. <https://doi.org/10.1145/3447548.3467430>
- [7] Shengnan Guo, Youfang Lin, Ning Feng, Chao Song, and Huaiyu Wan. 2019. Attention Based Spatial-Temporal Graph Convolutional Networks for Traffic Flow Forecasting. In *Proceedings of the AAAI Conference on Artificial Intelligence*, Vol. 33. 922–929. <https://doi.org/10.1609/aaai.v33i01.3301922>
- [8] Shengnan Guo, Youfang Lin, Huaiyu Wan, Xiucheng Li, and Gao Cong. 2021. Learning Dynamics and Heterogeneity of Spatial-Temporal Graph Data for Traffic Forecasting. *IEEE Transactions on Knowledge and Data Engineering* PP, 99 (2021), 1–1. <https://doi.org/10.1109/tkde.2021.3056502>
- [9] Liangzhe Han, Bowen Du, Leilei Sun, Yanjie Fu, Yisheng Lv, and Hui Xiong. 2021. Dynamic and Multi-Faceted Spatio-Temporal Deep Learning for Traffic Speed Forecasting. In *Proceedings of the 27th ACM SIGKDD Conference on Knowledge Discovery & Data Mining*. Association for Computing Machinery, New York, NY, USA, 547–555. <https://doi.org/10.1145/3447548.3467275>
- [10] Kaiming He, Xiangyu Zhang, Shaoqing Ren, and Jian Sun. 2016. Deep Residual Learning for Image Recognition. In *IEEE Conference on Computer Vision and Pattern Recognition*. 770–778. <https://doi.org/10.1109/CVPR.2016.90>
- [11] Sepp Hochreiter and Jürgen Schmidhuber. 1997. Long Short-Term Memory. *Neural Computation* 9, 8 (Nov. 1997), 1735–1780. <https://doi.org/10.1162/neco.1997.9.8.1735>
- [12] Young-Seon Jeong, Young-Ji Byon, Manoel Mendonca Castro-Neto, and Said M. Easa. 2013. Supervised Weighting-Online Learning Algorithm for Short-Term Traffic Flow Prediction. *IEEE Transactions on Intelligent Transportation Systems* 14, 4 (2013), 1700–1707. <https://doi.org/10.1109/TITS.2013.2267735>
- [13] Mengzhang Li and Zhanxing Zhu. 2021. Spatial-Temporal Fusion Graph Neural Networks for Traffic Flow Forecasting. In *Proceedings of the AAAI Conference on Artificial Intelligence*, Vol. 35. 4189–4196.
- [14] Yaguang Li, Rose Yu, Cyrus Shahabi, and Yan Liu. 2018. Diffusion Convolutional Recurrent Neural Network: Data-Driven Traffic Forecasting. In *International Conference on Learning Representations*.
- [15] Chi Harold Liu, Chengzhe Piao, Xiaoxin Ma, Ye Yuan, Jian Tang, Guoren Wang, and Kin K. Leung. 2021. Modeling Citywide Crowd Flows using Attentive Convolutional LSTM. In *IEEE International Conference on Data Engineering (ICDE)*. 217–228. <https://doi.org/10.1109/ICDE51399.2021.00026>
- [16] Zheng Lu, Chen Zhou, Jing Wu, Hao Jiang, and Songyue Cui. 2016. Integrating Granger Causality and Vector Auto-Regression for Traffic Prediction of Large-Scale WLANs. *KSII Transactions on Internet and Information Systems* 10, 1 (Jan. 2016), 136–151. <https://doi.org/10.3837/tiis.2016.01.008>
- [17] Xianglong Luo, Danyang Li, Yu Yang, and Shengrui Zhang. 2019. Spatiotemporal Traffic Flow Prediction with KNN and LSTM. *Journal of Advanced Transportation* 2019 (2019), 10. <https://doi.org/10.1155/2019/4145353>
- [18] David N. Reshef, Yakir A. Reshef, Hilary K. Finucane, Sharon R. Grossman, Gilean McVean, Peter J. Turnbaugh, Eric S. Lander, Michael Mitzenmacher, and Pardis C. Sabeti. 2011. Detecting Novel Associations in Large Data Sets. *Science* 334, 6062 (2011), 1518–1524. <https://doi.org/10.1126/science.1205438>
- [19] Chao Song, Youfang Lin, Shengnan Guo, and Huaiyu Wan. 2020. Spatial-Temporal Synchronous Graph Convolutional Networks: A New Framework for Spatial-Temporal Network Data Forecasting. In *Proceedings of the AAAI Conference on Artificial Intelligence*, Vol. 34. 914–921. <https://doi.org/10.1609/aaai.v34i01.5438>
- [20] Yuxing Sun, Biao Leng, and Wei Guan. 2015. A Novel Wavelet-SVM Short-Time Passenger Flow Prediction in Beijing Subway System. *Neurocomputing* 166, C (Oct. 2015), 109–121. <https://doi.org/10.1016/j.neucom.2015.03.085>
- [21] JWC Van Lint and CPJ Van Hinsbergen. 2012. Short-Term Traffic and Travel Time Prediction Models. *Artificial Intelligence Applications to Critical Transportation Issues* 22, 1 (2012), 22–41.
- [22] Ashish Vaswani, Noam Shazeer, Niki Parmar, Jakob Uszkoreit, Llion Jones, Aidan N. Gomez, Łukasz Kaiser, and Illia Polosukhin. 2017. Attention is All You Need. In *Proceedings of the 31st International Conference on Neural Information Processing Systems*. Curran Associates Inc., 6000–6010.
- [23] Jichen Wang, Weiguo Zhu, Yongqi Sun, and Chunzi Tian. 2021. An effective dynamic spatiotemporal framework with external features information for traffic prediction. *Applied Intelligence* 51, 6 (Jun. 2021), 3159–3173. <https://doi.org/10.1007/s10489-020-02043-1>
- [24] Yuandong Wang, Hongzhi Yin, Tong Chen, Chunyang Liu, Ben Wang, Tianyu Wo, and Jie Xu. 2021. Gallat: A Spatiotemporal Graph Attention Network for Passenger Demand Prediction. In *IEEE International Conference on Data Engineering (ICDE)*. 2129–2134. <https://doi.org/10.1109/ICDE51399.2021.00212>
- [25] Zonghan Wu, Shirui Pan, Guodong Long, Jing Jiang, Xiaoju Chang, and Chengqi Zhang. 2020. Connecting the Dots: Multivariate Time Series Forecasting with Graph Neural Networks. In *Proceedings of the 26th ACM SIGKDD International Conference on Knowledge Discovery & Data Mining*. 753–763. <https://doi.org/10.1145/3394486.3403118>
- [26] Zonghan Wu, Shirui Pan, Guodong Long, Jing Jiang, and Chengqi Zhang. 2019. Graph WaveNet for Deep Spatial-Temporal Graph Modeling. In *Proceedings of the International Joint Conference on Artificial Intelligence*, Sarit Kraus (Ed.). 1907–1913. <https://doi.org/10.24963/ijcai.2019/264>
- [27] Huaxiu Yao, Fei Wu, Jintao Ke, Xianfeng Tang, Yitian Jia, Siyu Lu, Pinghua Gong, Jieping Ye, and Zhenhui Li. 2018. Deep Multi-View Spatial-Temporal Network for Taxi Demand Prediction. In *Proceedings of the AAAI Conference on Artificial Intelligence*. 2588–2595.
- [28] Bing Yu, Haoteng Yin, and Zhanxing Zhu. 2018. Spatio-temporal Graph Convolutional Networks: A Deep Learning Framework for Traffic Forecasting. In *Proceedings of the International Joint Conference on Artificial Intelligence*.
- [29] Junbo Zhang, Yu Zheng, Dekang Qi, Ruiyuan Li, Xiuwen Yi, and Tianrui Li. 2018. Predicting Citywide Crowd Flows Using Deep Spatio-Temporal Residual Networks. *Artificial Intelligence* 259 (2018), 147–166.
- [30] Chuanpan Zheng, Xiaoliang Fan, Cheng Wang, and Jianzhong Qi. 2020. GMAN: A Graph Multi-Attention Network for Traffic Prediction. In *Proceedings of the AAAI Conference on Artificial Intelligence*, Vol. 34. 1234–1241. <https://doi.org/10.1609/aaai.v34i01.5477>

- [31] Xian Zhou, Yanyan Shen, Linpeng Huang, Tianzi Zang, and Yanmin Zhu. 2021. Multi-Level Attention Networks for Multi-Step Citywide Passenger Demands Prediction. *IEEE Transactions on Knowledge and Data Engineering* 33, 5 (2021), 2096–2108. <https://doi.org/10.1109/TKDE.2019.2948005>

## A APPENDIX REPRODUCIBILITY

In this section, the details of our implementation for reproducibility are provided. The source code, data, training logs and models can be found in the GitHub link<sup>1</sup>.

### A.1 Parameter Settings

Our model chooses the MAE loss function and Adam optimizer for training. We feed the historical data into the encoder and decoder networks during training. Once the decoder network generates prediction results, the optimizer adjusts the model parameters according to the training loss. We set the learning rate at 0.001, and other hyperparameters are described in Table 4. To compare all the baseline methods, we adopt three kinds of periodic traffic data (hourly, daily and weekly) to predict the traffic flow in the next hour. We set hourly, daily and weekly periodic traffic data for the highway traffic flow datasets, while we set hourly and daily periodic traffic data for the metro crowd flow datasets.

**Table 4: Hyperparameters of our CorrSTN model for four datasets.**

	#encoder layers	#decoder layers	#kernel size	#heads	#batchsize
PEMS07	3	3	3	8	4
PEMS07(p)	3	3	3	8	2
PEMS08	4	4	3	8	16
PEMS08(p)	4	4	3	8	8
HZME(in)	4	4	3	8	4
HZME(in)(p)	4	4	3	8	16
HZME(out)	3	3	5	4	8
HZME(out)(p)	4	4	3	4	16

### A.2 Metrics

We evaluate the performance of our model by the metrics of mean absolute error (MAE), root mean square error (RMSE) and mean absolute percentage error (MAPE). They are defined as,

$$\begin{aligned}
 \text{MAE}(\hat{X}^i, X^i) &= \frac{1}{L} \sum_{i=1}^L |X^i - \hat{X}^i| \\
 \text{RMSE}(\hat{X}^i, X^i) &= \sqrt{\frac{1}{L} \sum_{i=1}^L (X^i - \hat{X}^i)^2} \\
 \text{MAPE}(\hat{X}^i, X^i) &= \frac{1}{L} \sum_{i=1}^L \frac{|X^i - \hat{X}^i|}{X^i}.
 \end{aligned} \tag{17}$$

### A.3 Comparison on CIATT with different top U

In this subsection, we adopt six different  $U$  schemes on the HEME (inflow) dataset to verify the performance with different levels of spatial correlation information. We set  $U$  at 2, 3, 4, 5, 8 and 10, respectively, and the other hyperparameters are set as shown in Table 4.

<sup>1</sup><https://github.com/DrownFish19/CorrSTN>

As shown in Figure 7, one can clearly see that the CorrSTN model achieves the best result when  $U$  is set at 4 on the HEME (inflow) dataset. Another phenomenon is that as  $U$  increases from 2, the metrics of MAE, RMSE and MAPE gradually decrease until  $U = 4$ , and then the metrics continue to increase. This indicates that spatial correlation information representations among the sensors are effective and that the top  $U$  selection operator is necessary for CIATT.

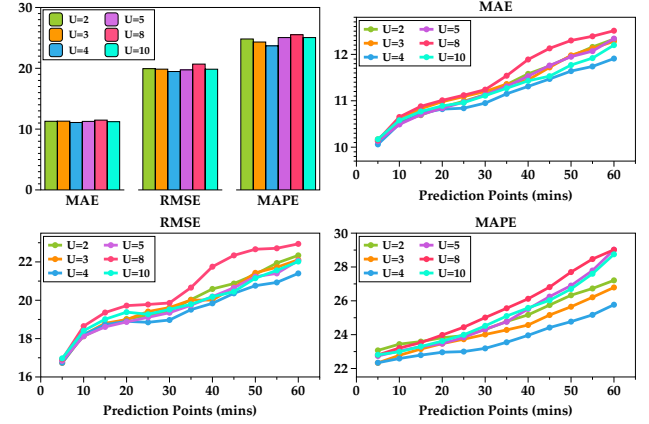


**Figure 7: Results on the HZME (inflow) dataset with six different  $U$  schemes.**

### A.4 Comparison on the static and dynamic SCorr

In this subsection, we compare static and dynamic types of SCorr on the HZME (inflow) dataset. The dynamic SCorr is calculated by Equation (4) with  $T$  at 12 timestamps (one hour) and cyclic forwarding along the timeline. Initially, we suppose that dynamic SCorr is better than static SCorr. However, CorrSTN with static SCorr achieves markedly better results than CorrSTN with dynamic SCorr, as shown in Figure 8.

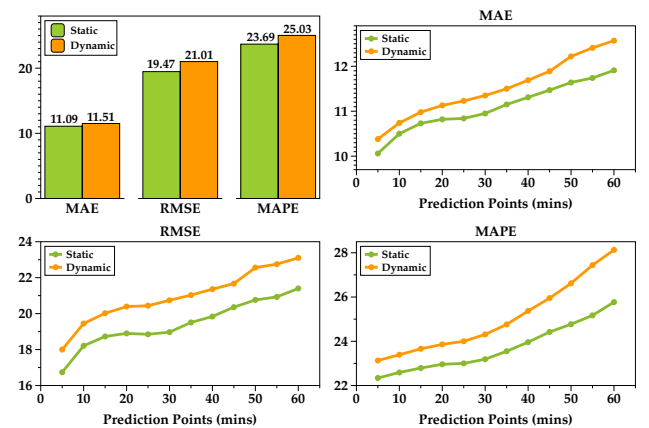


**Figure 8: Results on the HZME (inflow) dataset with static and dynamic spatial correlation information.**

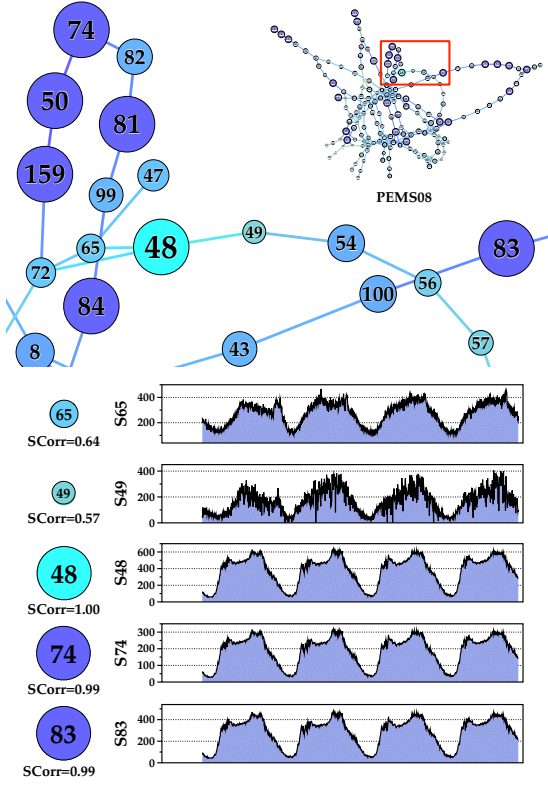


Figure 9: The spatial correlation information between sensor 48 and other sensors on the PEMS08 dataset.

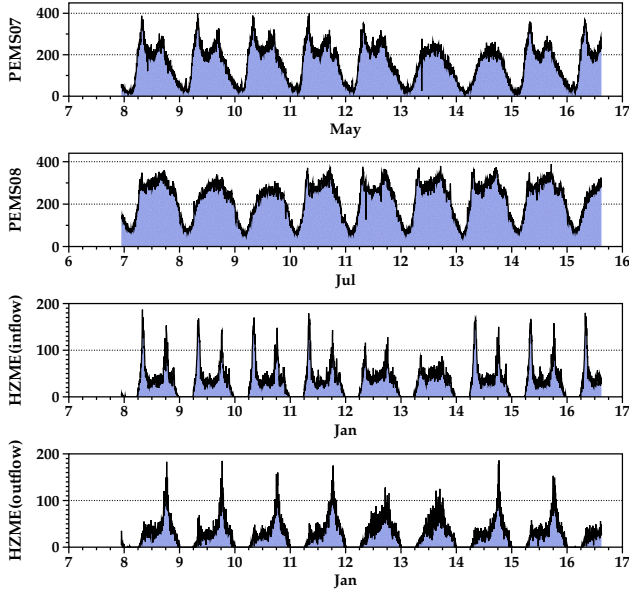


Figure 10: The original data on the PEMS07, PEMS08, HZME (inflow) and HZME (outflow) datasets.

In our opinion, although the dynamic SCorr contains rich information at each time point, the high-frequency change in SCorr makes the model hard to fit all training data. In addition, the correlative relationships will not always change in fact. Thus, the predictive performance of static SCorr outperforms the performance of dynamic SCorr.

### A.5 Time Complexity

We implement the proposed model in Python 3.8 and PyTorch 1.7.0. The model has been successfully executed and tested on the Linux platform with an Intel (R) Xeon (R) Gold 6240R CPU@2.40 GHz and NVIDIA TESLA V100 (PCI-E) GPU 32 GB card. We list the time cost of SCorr and TCorr (CPU: AMD 3970x 32C64T). The time cost of SCorr can be reduced with more parallel computing cores. Moreover, TCorr can accurately make the best data selection scheme in 18s, while the neural network cannot finish the one epoch training simultaneously.

Table 5: Training and test time on four datasets.

	SCorr Time Cost	TCorr Time Cost
PEMS07	04:42:00	00:00:18
PEMS08	00:20:00	00:00:02
HZME(inflow)	00:00:17	<00:00:01
HZME(outflow)	00:00:17	<00:00:01

## B CASE STUDY

In this section, we provide details of SCorr and TCorr on the real-world datasets.

### B.1 The Case Study of SCorr

In the traffic flow data, correlation information exists among sensors of different traffic networks. Taking the PEMS08 dataset as an example, we calculate the correlation of sensors by using SCorr, as shown in Figure 9, where the size of each sensor indicates its correlation degree with sensor 48. Both sensor 74 and sensor 83 have strong correlation representations with sensor 48, although there are no structural paths among them directly. The counterintuitive phenomenon shows that correlation information is more significant than structural information for discovering spatiotemporal dependencies and dynamic relationships in traffic forecasting. Furthermore, according to the sensor 48 sequence and four other sequences, we find that SCorr can accurately capture a wider range of associations and provide a precise value to evaluate the correlation strength.

### B.2 The Case Study of TCorr

To verify the characteristics of each dataset, we illustrate the original data, as shown in Figure 10. The PEMS07 and PEMS08 datasets have a stronger correlation with the weekly data than with the daily data. However, the HZME inflow and outflow datasets are opposite. Thus, the different characteristics prove the correctness of TCorr and the effectiveness of different data selection schemes.